Section 2

ADVANCED TECHNOLOGY DEVELOPMENTS

2.A Anticipated Improvement in Laser-Beam Uniformity Using Distributed Phase Plates with Quasi-Random Patterns

Distributed phase plates (DPP's)[1,2] have been used at LLE[3] to improve laser-irradiation uniformity on target. We will show that uniformity can be further improved by using DPP's where the spatial correlations in the pattern of phase elements have been reduced, relative to the correlations that would occur fortuitously in random patterns. Diffraction theory[4] shows that the size and wavelength of the nonuniformity are determined by spatial correlations in the phase distribution of the beam. Long-wavelength nonuniformities in the intensity distribution, which are relatively difficult to overcome in the target by thermal smoothing and in the laser by, e.g., spectral dispersion (SSD),[5] result from short-length correlations in the phase distribution of the beam. We have constructed DPP patterns with smaller short-range correlations than would occur randomly. Calculations show that if variations in the intrinsic phase error of a beam over short distances in the aperture plane are sufficiently small, then a "reduced-correlation" DPP will produce a net phase distribution with correlations over these separations that are also less than would occur randomly. As a result, the long-wavelength nonuniformities in single-beam intensity patterns can be reduced with these masks. We will show how the degree of improvement depends on the intrinsic phase error of the beam. We will also show the effect of this improvement on the uniformity of spherical illumination by multibeam systems.

A random two-level DPP is a flat, transparent plate divided into a large number of identical area elements, except that half of them, chosen at random, add a half-wave delay to the transmitted light.[1] At present, the random DPP's on the OMEGA laser system, illustrated in Fig. 40.9, use elements shaped as regular hexagons.[3] Without a DPP, the target is placed within the converging focused beam at the point on the axis where the beam illuminates a full hemisphere. This gives an intensity distribution on target with large, long-scale modulations caused by phase nonuniformities in the beam.[6] With a DPP in the beam as shown in Fig. 40.9, the random phase distribution effectively divides the beam into beamlets that focus onto the target within an area determined by the diffraction limit of the individual mask element. The element size is chosen so that the diffraction-limited focal spot of an individual beamlet matches the target diameter. As evident in Fig. 40.10, the interference among the beamlets produces modulation that is much finer and much more easily smoothed in the target and in the laser itself, e.g., by induced spatial incoherence (ISI)[7] or by SSD.[5]

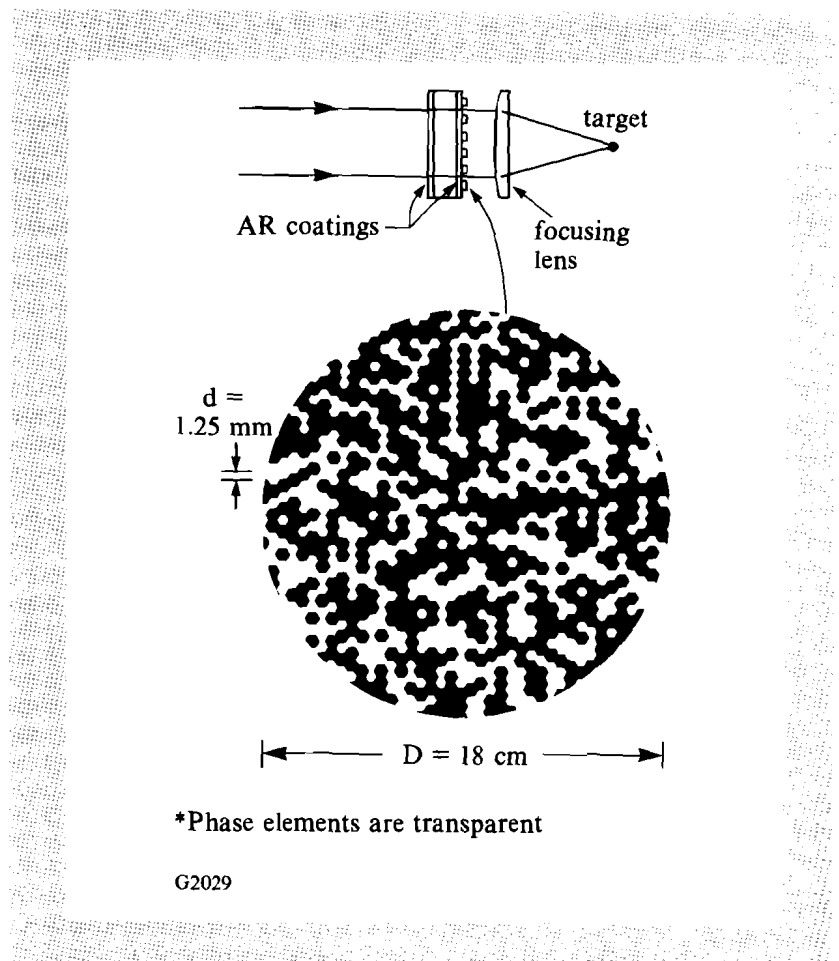*Phase elements are transparent

G2029

Fig. 40.9
DPP's in current use on the OMEGA laser system are regular arrays of hexagonal area elements, half of which, chosen at random, impart a half-wave phase delay to the passing light.

The functional form of the intensity distribution resulting from using a DPP can be expressed as the smooth, ideally uniform intensity distribution of the individual DPP element, multiplied by a modulating function of the form of a Fourier series with coefficients equal to values of the correlation function of the profile beam's net phase distribution $\phi(\vec{x})$ after passing through the DPP. The oscillations of the modulation function account for the beam nonuniformity, so the uniformity can be improved if the correlation function can be reduced. If the intrinsic phase error of the beam is sufficiently constant over a given distance in the near-field plane, then correlations in the net phase over this distance can be reduced by altering the correlation properties of the DPP. The critical limitation is the phase error in the beam. If it is large, compared with about a quarter wave over a given scale length, then the correlation properties of the DPP over that scale length will be overwhelmed by the intrinsic phase distribution of the beam.

The relationship between the nonuniformity of the focused illumination and the correlation properties of the net phase distribution of the beam can be obtained from the Fraunhofer equation for the diffraction of a signal field $U(\vec{q})$ of total energy E per unit time and wavelength λ irradiating an aperture of area A,

$$U(\vec{q}) = \frac{1}{\lambda R} \sqrt{\frac{E}{A}} \iint_A W(\vec{x}) \, e^{-i[\vec{q}\cdot\vec{x} + \phi(\vec{x})]} d^2x , \qquad (1a)$$

where $W(\vec{x})$ is the amplitude distribution in the aperture plane, normalized so that

$$\iint_A W^2(\vec{x}) \, d^2x = A , \qquad (1b)$$

and where $\phi(\vec{x})$ is the sum of the intrinsic phase distribution of the beam plus the phase added by the DPP.[4] The vector $\vec{x}$ is a point in the aperture plane, $\vec{q}$ is the wave vector of the diffracted signal, and R is the distance from the aperture plane to the image plane. The amplitude distribution $W(\vec{x})$ is zero everywhere outside the illuminated portion of the aperture.

Dividing the aperture into N identical elements of area $a = A/N$, Eq. (1a) becomes

$$U(\vec{q}) = \frac{1}{\lambda R} \sqrt{\frac{E}{A}} \iint_a e^{-i\vec{q}\cdot\vec{\xi}} \, d^2\xi \times \sum_{j=1}^{N} W(\vec{x}_j) \, e^{-i[\vec{q}\cdot\vec{x}_j + \phi(x_j)]} , \qquad (2)$$

where it is assumed that the amplitude weight and the intrinsic phase error of the beam vary slowly enough to be considered constant over each element. The vector $\vec{\xi}$ is the position within an element, relative

to $\vec{x}_j$, the position (e.g., centroid) of the jth element. The intensity calculated from this expression is of the form

$$I(\vec{q}) = |U(\vec{q})|^2 = N \, I_0(\vec{q}) \, G(\vec{q}) \ , \tag{3a}$$

where

$$I_0(\vec{q}) = \frac{E}{\lambda^2 R^2 A} \left| \iint_a e^{-i\vec{q}\cdot\vec{\xi}} \, d^2\xi \right|^2 . \tag{3b}$$

The form is that of the diffraction-limited intensity distribution of the individual element, $I_0(\vec{q})$, modulated by the function

$$G(\vec{q}) = 1 + \sum_{\Delta\vec{x}\in S} e^{-i\vec{q}\cdot\Delta\vec{x}} \, C(\Delta\vec{x}), \tag{3c}$$

where

$$C(\Delta\vec{x}) = \frac{1}{N} \sum_{k=1}^{N} W(\vec{x}_k) W(\vec{x}_k + \Delta\vec{x}) \, e^{i[\phi(\vec{x}_k) - \phi(\vec{x}_k + \Delta\vec{x})]} , \tag{3d}$$

which is of the form of a Fourier series with coefficients given by the correlation function $C(\Delta\vec{x})$ of the phase distribution $\phi(\vec{x})$. The summation in Eq. (3c) is taken over all vectors in the set $S \equiv \{\Delta\vec{x}_{jk}\}$, the set of all distinct inter-element displacement vectors, $\Delta\vec{x}_{jk} \equiv \vec{x}_j - \vec{x}_k$. From Eq. (3d), it is clear that reducing spatial correlations in the net phase distribution will reduce the modulation of the focused intensity distribution. Even though Eqs. (3a)–(3d) are general enough to include a nonuniform amplitude distribution in the incident beam, a uniform distribution will be assumed in all computed examples to follow. To a good degree of accuracy, this is consistent with what has been achieved.[6]

The form of the intensity distribution and the modulation function is clearer in the one-dimensional case. For a DPP of length L with N elements, the intensity distribution takes the form

$$I(p) = N \, I_0(p) \, G(p) \ , \tag{4a}$$

where the smooth profile

$$I_0(p) = \frac{EL}{\lambda RN} \, \frac{sin^2\theta}{\theta^2} \tag{4b}$$

is modulated by the function

$$G(p) = 1 + \sum_{n=1}^{N-1} [g_n \, cos \, 2n\theta + h_n \, sin \, 2n\theta] \ , \tag{4c}$$

where the diffraction angle p is given by

$$p = \frac{\lambda N\theta}{\pi L} \quad .$$ (4d)

For the case of a plane wave incident on a DPP, the intrinsic phase error of the beam is zero, so $\phi(\vec{x}_j) = \phi_j$, the intrinsic phase alone, which is 0 or π, and one obtains $h_n = 0$ and

$$g_n = \frac{2}{N} \sum_{j=1}^{N-n} \cos\phi_j \; \cos\phi_{j+n} \quad ,$$ (5)

If the phases of the DPP elements $\{\phi_j\}$ are chosen at random, then this quantity generally follows the root-N statistics of accumulated random steps,[8]

$$|g_n| \approx \frac{2\sqrt{N-n}}{N}$$ (6)

but smaller values can be obtained if the DPP element phases are chosen appropriately.

Construction of a reduced-correlation pattern proceeds by setting the phase of each element, one at a time, to the value that minimizes a predefined measure of correlation among all the previously defined elements. The construction begins from a small (e.g., 2 × 2) seed array. The correlation measure to be minimized is the square of the correlation function of all the defined elements, summed over the domain of correlation reduction, which can be any subset of $\{\Delta \vec{x}_{jk}\}$, the set of interelement displacements. One such measure is given by

$$Q(n_0) = \sum_{n=1}^{n_0} G_n^2 \quad ,$$ (7a)

where

$$G_n^2 = \sum_{\Delta \vec{x} \in S_n} |C(\Delta \vec{x})|^2 \quad .$$ (7b)

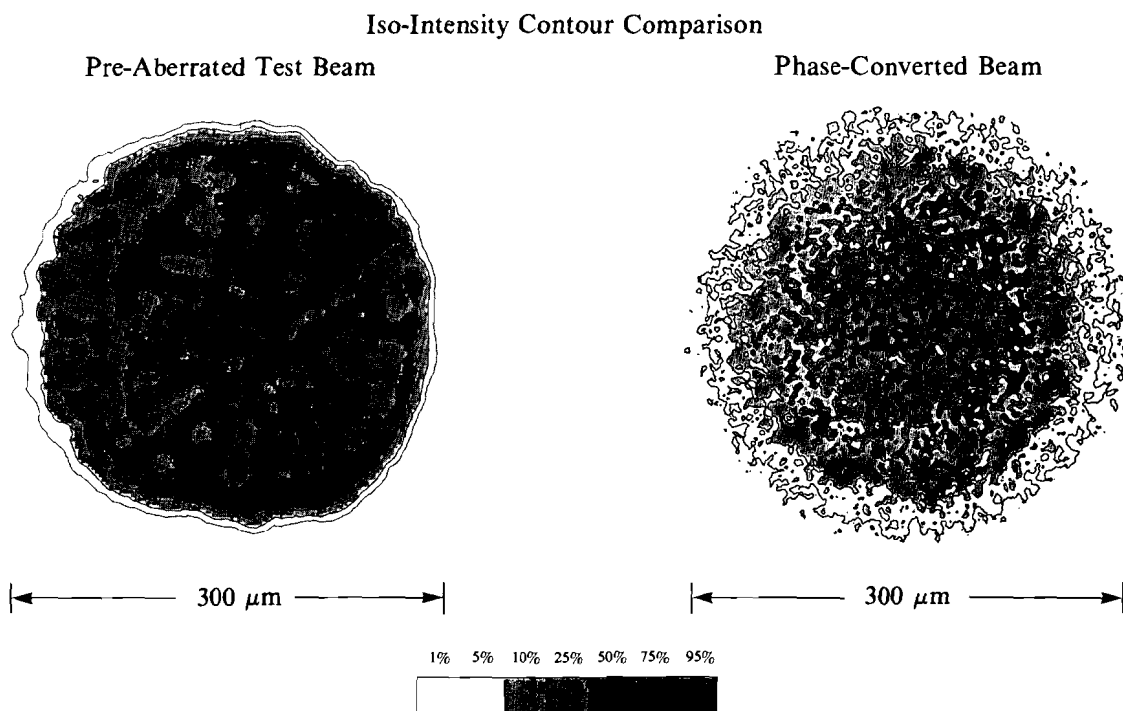The summation in this expression is taken over

$$S_n \quad \{\Delta \vec{x}_{jk} | n \geq |\Delta \vec{x}_{jk}| > n-1\} \quad ,$$

the subset of all distinct displacement vectors that fall within the specified range of length. Equation (7b) is evaluated only in terms of the defined pattern elements. The parameter n_0 defines the domain, or "range," of correlation reduction expressed in units of the period of the DPP pattern's underlying lattice. The quantity G_n is a direction average of the autocorrelation function over a unit range of separations. For this criterion, then, the domain of correlation

reduction is the set of all separations, up to n_0 "elements" or array spacings. In the case of the one-dimensional DPP, we have $G_n = g_n$, and this criterion reduces to that of minimizing the quantity

$$Q(n_0) = \sum_{n=1}^{n_0} |g_n|^2 .$$ (8)

If the choice of phase for an element is indeterminate, then the setting is made that tends to equalize the number of elements among the possible choices. The patterns we obtain are completely random in appearance, but they are not random because their correlation properties are not those of random patterns.

Iso-Intensity Contour Comparison

Pre-Aberrated Test Beam   Phase-Converted Beam

|◄——— 300 μm ———►| |◄——— 300 μm ———►|

1% 5% 10% 25% 50% 75% 95%

G2141

Fig. 40.10
The phase redistribution by a DPP converts a beam that can produce, at best, a coarsely modulated illumination pattern into a beam whose focused illumination pattern has the form of a high-intensity, short-scale structure superimposed upon a smooth diffraction-limited distribution of a single element.

This construction method is easily generalized to any regular array of a single equilateral or stretched shape that can completely tile a surface, such as, in the case of OMEGA,[3] hexagons. Also, more than two phase levels can be considered,[9] and any domain of correlation

reduction can be chosen. Modulations of any wavelength and orientation can be reduced, as long as the corresponding set of correlation displacements can be identified.

Elements need not be chosen in any particular order, other than that each new element should be contiguous to the previously set elements. This causes the choice of phase for the new element to be based on correlations with as many previously set elements as possible. At any stage in the construction, the set of defined elements should completely cover the area enclosed by a reasonably smooth, simple closed boundary. Since the correlations over the domain of correlation reduction are kept low throughout the construction of the pattern, as the area grows, the pattern has the desirable property that any piece of it also has reduced-correlation properties. Appropriate terminology for this property is "local nonredundancy" because the repetitiveness of the pattern found in any neighborhood in the pattern is less pronounced than the fortuitous repetition typical of a random pattern. Thus, one can expect improved uniformity, even if only a part of the DPP is illuminated or the illumination of the aperture is not perfectly uniform. In choosing possible DPP patterns, the preservation of reduced spatial correlations for a realistic variety of aperture illuminations can be an important consideration.

Lower autocorrelation values overall are obtained if the pattern is constructed only within the portion of the aperture to be illuminated because then the phase settings of the elements are not biased by their correlations with irrelevant, unilluminated elements. Iterating the pattern construction does give a slight additional reduction in correlations, but since all the phase elements have been set in the first iteration, the figure of merit becomes the sum over the entire pattern. Consequently, additional reduction in the figure of merit can come at the cost of degrading the local nonredundancy. The benefits and drawbacks of iteration and adjustments in the domain of the correlation reduction are best considered in the context of a specific application. If bench tests of reduced-correlation DPP's are sufficiently encouraging, further optimization will be undertaken.
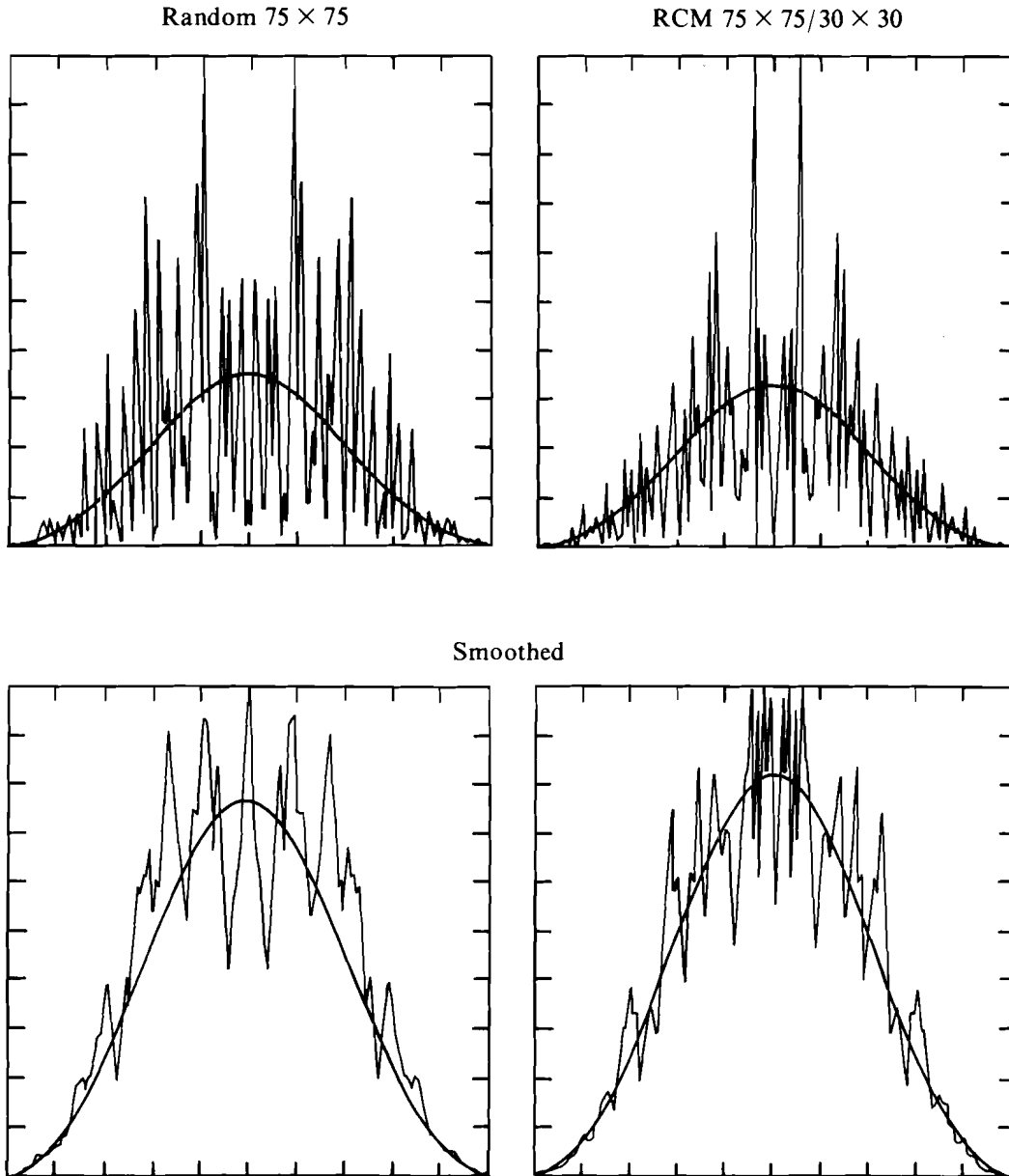
To date, there has been no reported application of nonrandom patterns to DPP technology, so far as we are aware, but it has been anticipated for many years that arrays with controlled correlation properties would be useful in optical signal processing and pattern recognition.[10] For example, "pseudo-noise arrays"[11] have been developed[12,13] as the imaging elements in x-ray and gamma-ray optics.[14] Construction of arrays can proceed according to number-theoretical methods[10,11] as well as by choice, one element at a time, according to some criterion.[15] In this work, we have employed element-by-element construction because it offers much greater flexibility in array shape and size and, as was discussed above, a tolerance for variations in which a portion of the DPP is illuminated. The known pseudo-noise arrays are rectangular patterns of restricted dimensions. They must be formed into periodic mosaics, not only to form masks of a desired size and arrays of a desired total dimension, but also because their characteristic correlation functions are defined in

terms of cyclic sums that apply specifically to periodic arrays, rather than to a single array. Some pseudo-noise arrays are characterized by their correlations with special decoding arrays, rather than in terms of autocorrelations,[12,13] and these arrays obviously cannot be used in DPP's. Progress in relaxing dimension restrictions has been made,[13] but the resulting arrays contain many more elements of one value than the other, which leads to undesirable coherent-interference effects in the irradiation distribution. In spite of these difficulties, the possibility that the existing theory of pseudo-noise arrays might lead to arrays that are advantageous as DPP patterns deserves attention.

Examples of intensity distributions shown in this article are obtained by numerically evaluating Eqs. (1) and (3) in terms of net phase distributions.[16] In all cases, square DPP grids of various dimensions are assumed, and it will be made clear in each example whether the net phase includes the DPP contribution alone, or whether an assumed intrinsic phase error is included. In Fig. 40.11, the first example shows, by comparison, the effect of reducing correlations up to separations of 30 times the grid spacing in a DPP of dimension 75 × 75. The aperture is the inscribed circular area of the square array. The intensity profile along one axis of the intensity distribution is shown. The smooth curve in each frame is the ideal unmodulated profile given by Eqs. (3a) and (3b) for the case $G(\vec{q}) = 1$. To allow the long-wavelength modulations to be seen more clearly, a numerical smoothing over about 1% of the profile width has been applied in the corresponding lower frames. With short-range correlations in the DPP reduced, the long-scale modulations of the profile are noticeably smaller.

The quantity G_n given by Eq. (7b) is a useful measure of the autocorrelation spectrum that can be plotted as a function of n to show the distribution of modulation amplitude as a function of spatial frequency. Roughly speaking, G_n includes spatial frequencies from $2(n - 1)$ to $2n$ modulation periods within the central lobe of the profile width. Comparing plots of G_n versus n usually gives a better visualization of modulation reduction than comparisons of irradiation profiles.

In Fig. 40.12, G_n is plotted for the phase distributions of three different square (40 × 40) reduced-correlation DPP's and a random DPP. The reductions in autocorrelation relative to the random DPP are clearly seen for each of the three different ranges. Here, as in every other instance considered, with or without background phase error, correlations do not increase for separations over which correlations were not reduced. This is very important not only because it makes improved uniformity possible, but it is also not necessarily the expected result. Since the choice of a single-element phase affects the autocorrelation function for all separations up to the furthest-removed boundary element, reducing correlations over one range of separations affects correlations at other separations; we are aware of no reason why correlations over displacements not included in the choice criterion are not enhanced. Fortunately, correlation reduction does not appear to introduce correlations at any separation that are stronger than

Random 75 × 75

RCM 75 × 75/30 × 30

Smoothed

TC2596

Fig. 40.11

A pair of profiles of simulated intensity distributions given by 75 × 75 DPP's illustrates the effect of reducing correlations at separations of up to 30 elements. The ideal unmodulated intensity profile is superimposed for comparison. By reducing longer-wavelength modulations, correlation reduction causes the modulation to follow the ideal profile more closely. The two profiles are repeated below with a smoothing over about 1% of the profile width to allow easier comparison of the longer-wavelength modulations.

Fig. 40.12
The autocorrelation spectrum is plotted for 4 different 40 × 40 patterns. Lower correlations are obtained up to the correlation-reduction range and correlations outside this range are not increased above the level for a random pattern.
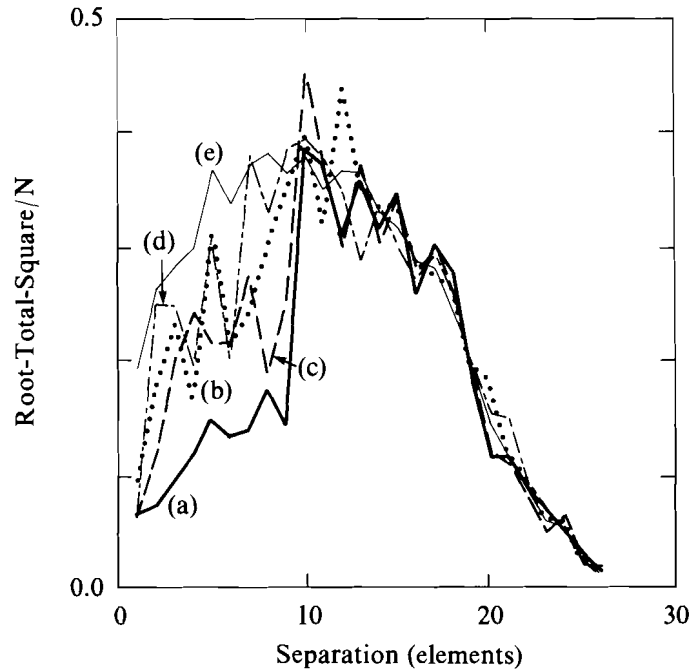
those that typically occur in random DPP's, which suggests that reduced-correlation DPP's can always be expected to perform better than random ones.

Correlation reduction in partially illuminated DPP's is demonstrated in Fig. 40.13 by comparing the autocorrelation spectra of five DPP's, each of dimension 20 × 20 and filling the same square aperture. The four patterns represented by curves (a)–(d) were all constructed with a correlation-reduction range of 10. Curve (a) represents a DPP array constructed only within the aperture. Curves (b)–(d) represent DPP's that are the center 20 × 20 sections of larger arrays of dimension 30 × 30, 40 × 40, and 50 × 50, respectively. All are to be compared with the random DPP represented by curve (e). Sizeable fluctuations in the correlations are caused by the relatively small number of elements in the illuminated pattern. The curve for the random case is an average spectrum derived statistically from the square root of the number of element pairs that fall within each separation bin. Consequently, it appears smoother than the other curves. Curves (a)–(d) all show correlations reduced below random levels, and, as was explained above, the correlation reduction is distinctly better in the pattern constructed only within the aperture.

An important question to consider is the degree of improvement obtained when the net phase distribution of the beam emerging from the DPP includes a typical level of phase error from the beam itself. The intrinsic phase distribution of the beam in the aperture plane is the critical limitation on the improvement in uniformity that can be
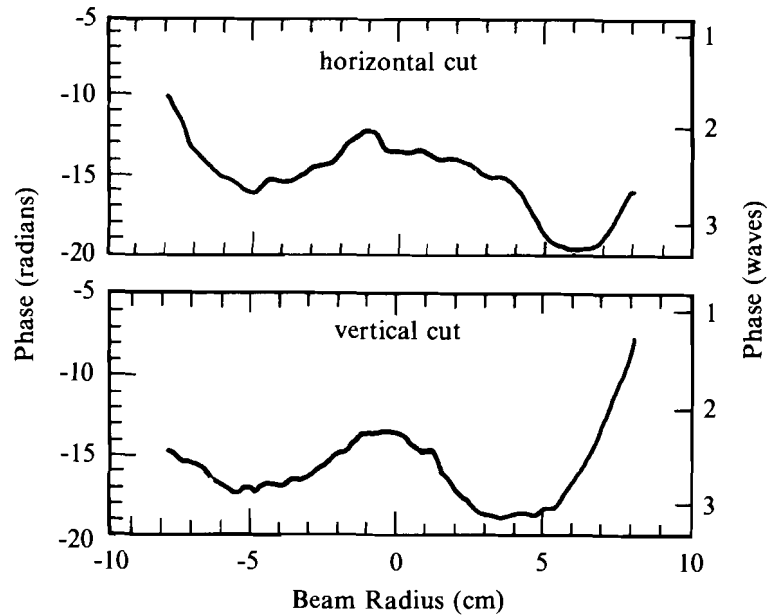
Fig. 40.13
Autocorrelation sums for five different DPP's are plotted. The range of correlation reduction in each case is 10, and the illuminated area is the entire 20 × 20 array. Curve (a) is derived from the pattern constructed only within the illuminated area. Curves (b)–(d) represent illuminated areas that are the center portions of larger patterns (30 × 30, 40 × 40, and 50 × 50, respectively), and curve (e) is the crude statistical result for a random pattern. While the greatest reduction of correlations occurs when the pattern is constructed only within the illuminated area, reduction is also obtained when only a small part of the aperture is illuminated.

obtained using reduced-correlation DPP's. For the purposes of this discussion, we will take the measured phase distribution of one beam of the OMEGA laser as typical.[6] This beam was chosen in advance of the phase measurement for its relatively good near-field amplitude uniformity, which is not necessarily a predictor of good phase uniformity. Profiles of this phase distribution along two orthogonal axes are plotted in Fig. 40.14. The effect of this typical intrinsic phase on focused intensity distributions is shown by the examples in Fig. 40.15. In these simulations, DPP's of dimension 75 × 75 were assumed, and a correlation-reduction range of ten grid spacings was used in the correlation-reduction case. Profiles along two orthogonal axes are shown. As in the bottom frames of Fig. 40.11, the profiles here are smoothed over about 1% of the beam radius. Even with the typical phase error in the beam, the focused-intensity profiles are noticeably improved with a reduced-correlation DPP.

As the intrinsic phase error of a beam is increased, the spatial-autocorrelation spectrum of net phase distribution begins to lose the nonrandom character of the DPP phase distribution. This is illustrated in Fig. 40.16 using a DPP pattern of dimension 100 × 100 and a correlation-reduction range of 30. At distances over which the intrinsic phase error varies by about a quarter wave, the half-wave contribution of the DPP to the net phase is obscured. At shorter separations where the phase error changes by a small fraction of a wave, the nonrandom correlation is left largely intact. Consequently, as the phase error is increased, degradation of the correlation reduction occurs first at the
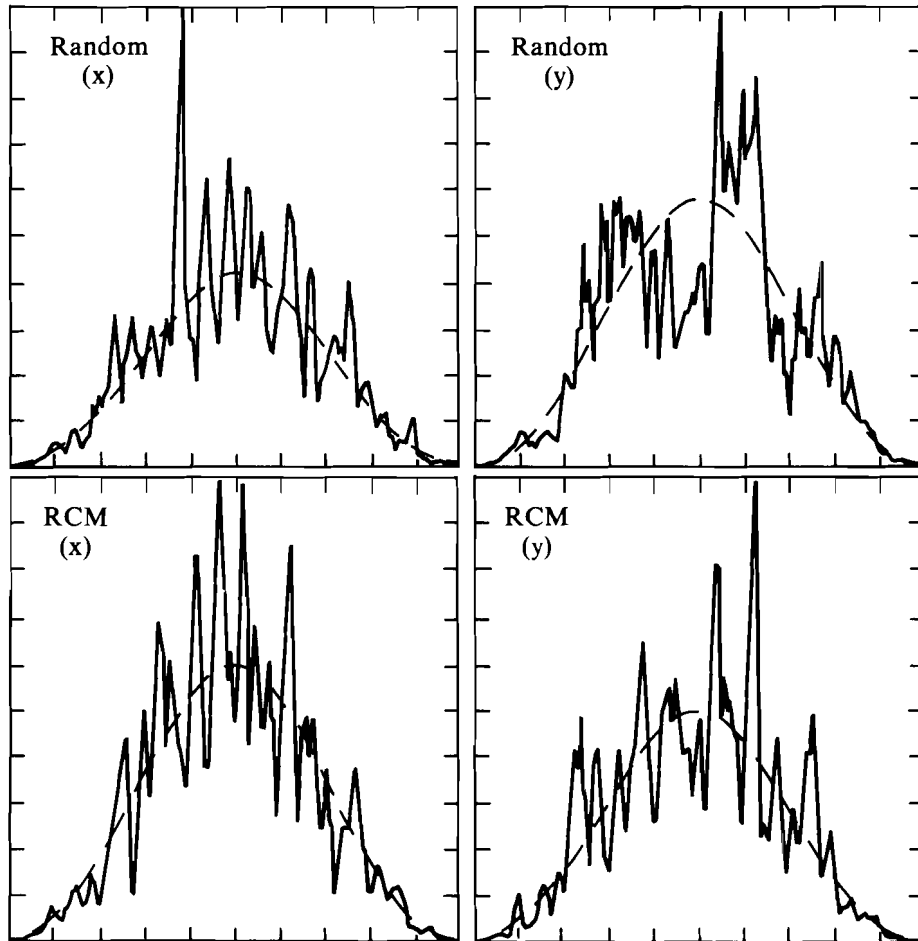
195

TC2187

Fig. 40.14
The measured intrinsic phase error for a typical OMEGA beam is plotted along
two axes of the aperture plane.

longer separations. Correlation reduction at the shortest separations,
those corresponding to the long-scale illumination nonuniformities, is
least affected by the phase error of the beam. As a result, substantial
improvement at these longer wavelengths is still obtained with the full
level of typical phase error. This gives hope that improvement in long-
wavelength uniformity might be possible in future experiments. Figure
40.17 includes a magnified detail of the short-range autocorrelation of
the net phase. Again, it is important to note that the contribution of the
intrinsic phase error does not increase the correlations of the net phase
above random levels.

The performance of ICF targets depends on the magnitude and
spatial-wavelength content of the irradiation nonuniformity on a
spherical surface.[17] The nonuniformity of the spherical irradiation has
been calculated for the 24-beam distribution used on the OMEGA laser
system in terms of a single-beam irradiance distribution, plus a random
rotation, at the appropriate positions on a sphere representing the
target surface. The resulting spherical-illumination pattern is
decomposed into spherical harmonics to examine the spatial-
wavelength content of the nonuniformity on target.[16] Two spherical-
mode decompositions of the illumination nonuniformity obtained using
reduced-correlation DPP's, with and without the typical phase error,
are shown as bar graphs of the modal amplitude in Fig. 40.18. DPP's
of 75 × 75 elements with a correlation-reduction range of 30 grid
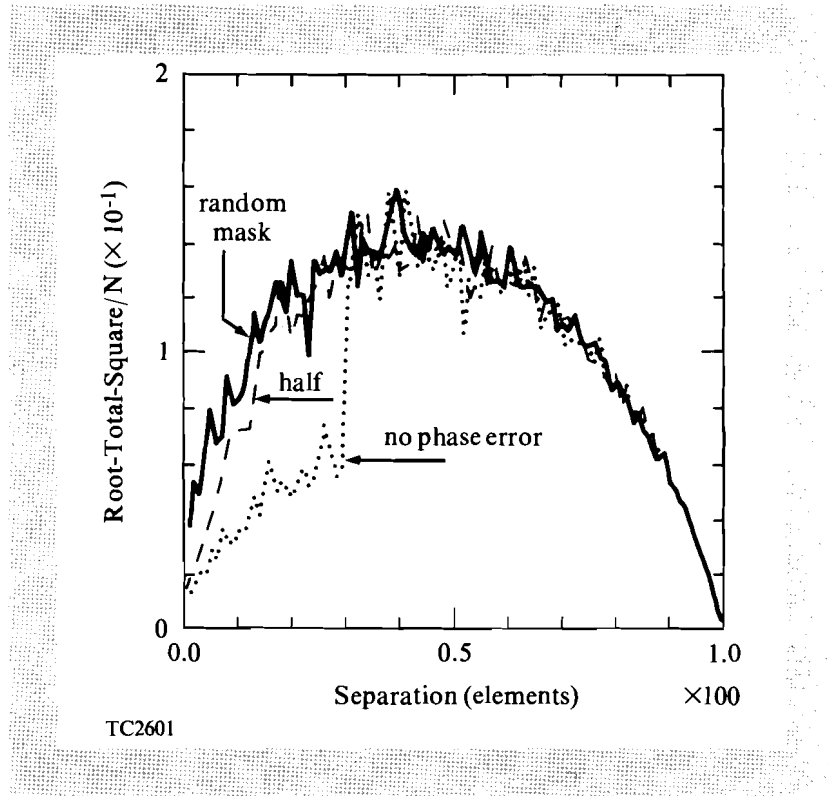
TC2587

Fig. 40.15
Orthogonal profiles of a simulated intensity distribution for 75 × 75 DPP's, including the effect of the "typical" phase error shown in Fig. 40.14. Correlations have been reduced up to a range of 10. A lower level of modulation, particularly at longer wavelengths, is seen using the reduced-correlation DPP's.

spacings were assumed. The improvement resulting from correlation reduction is seen by comparing the bar height with the solid curve, which represents an average of three simulations done with random DPP's. Improvement is obtained throughout the mode spectrum for the case of no phase error, while significant and repeatable improvement is seen only for modes up to $\ell \approx 7$ for the case including phase error. The deviation of the "random" curve from the amplitudes of higher modes, say $\ell \geq 20$, is indicative of the level of chance variations due to the use of differently seeded DPP's, different orientations of the beams, and different relative orientations of the DPP phase profile and the intrinsic phase distribution of the beam, all of which were varied in
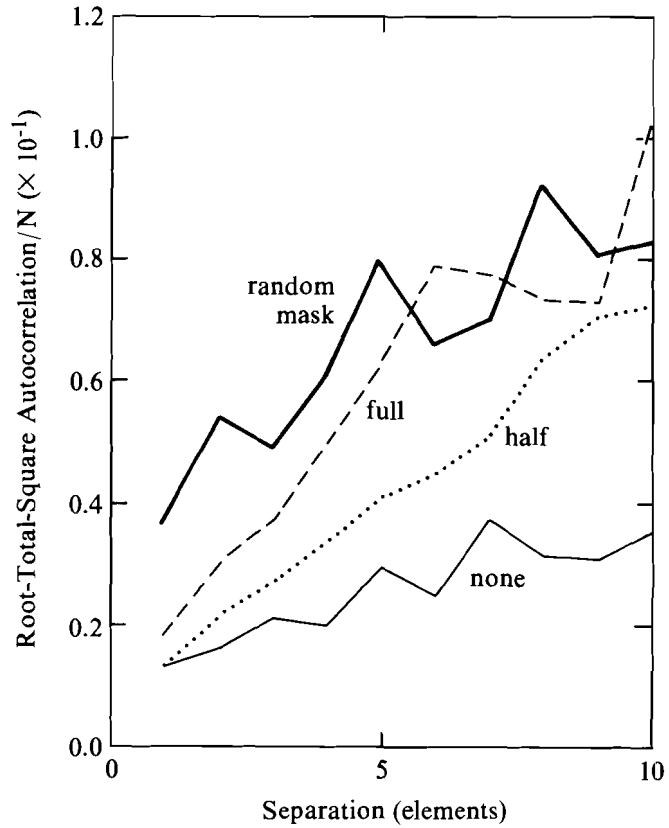
197

Fig. 40.16
The effect of phase error is seen in this comparison of autocorrelation functions of the net phase with a 100 × 100 DPP for various multiples of the "typical" phase-error distribution. Correlations in the DPP are reduced up to a range of 30 elements. As the phase error increases, correlations are randomized for all but the shortest separations.

the simulations. The solid segments in the bar graphs are the mode amplitudes that would be obtained for perfect, unmodulated beams.

To more clearly see the potential decrease in long-scale nonuniformity by applying reduced-correlation DPP's to a 24-beam system, the root-total-square nonuniformity of the first five modes is plotted in Fig. 40.19 in histograms of the simulations done to date. Again, DPP's of dimension 75 × 75 and correlation-reduction range 30 were assumed. To facilitate comparison, separate histograms are shown for perfect beams [$G(\vec{q}) = 1$], for reduced-correlation DPP's, and for random DPP's. Differences among simulations of the same type are explained above. The range of improvement using correlation reduction is comparable to the effect of a random 4%-rms beam-to-beam energy imbalance that was introduced into a few of the simulations indicated in order to allow comparison of correlation effects with a relatively well-understood source of illumination nonuniformity. The histograms suggest a possible distribution of outcomes, which gives a sense of how "lucky" or "unlucky" one might be with a given DPP and beam. In practice, the distribution will be somewhat narrower because the intrinsic phase distribution will vary from beam to beam, which will allow the natural random variability of results to average out more than in the simulations where the net phase profiles vary only by a random rotation. On the OMEGA system, the aperture, focal length, and target size require DPP arrays roughly a factor of 2 larger than the 75 × 75 square arrays assumed in the simulation, and the results could differ slightly. With an array of larger dimensions, a given modulation mode [e.g., a single term in
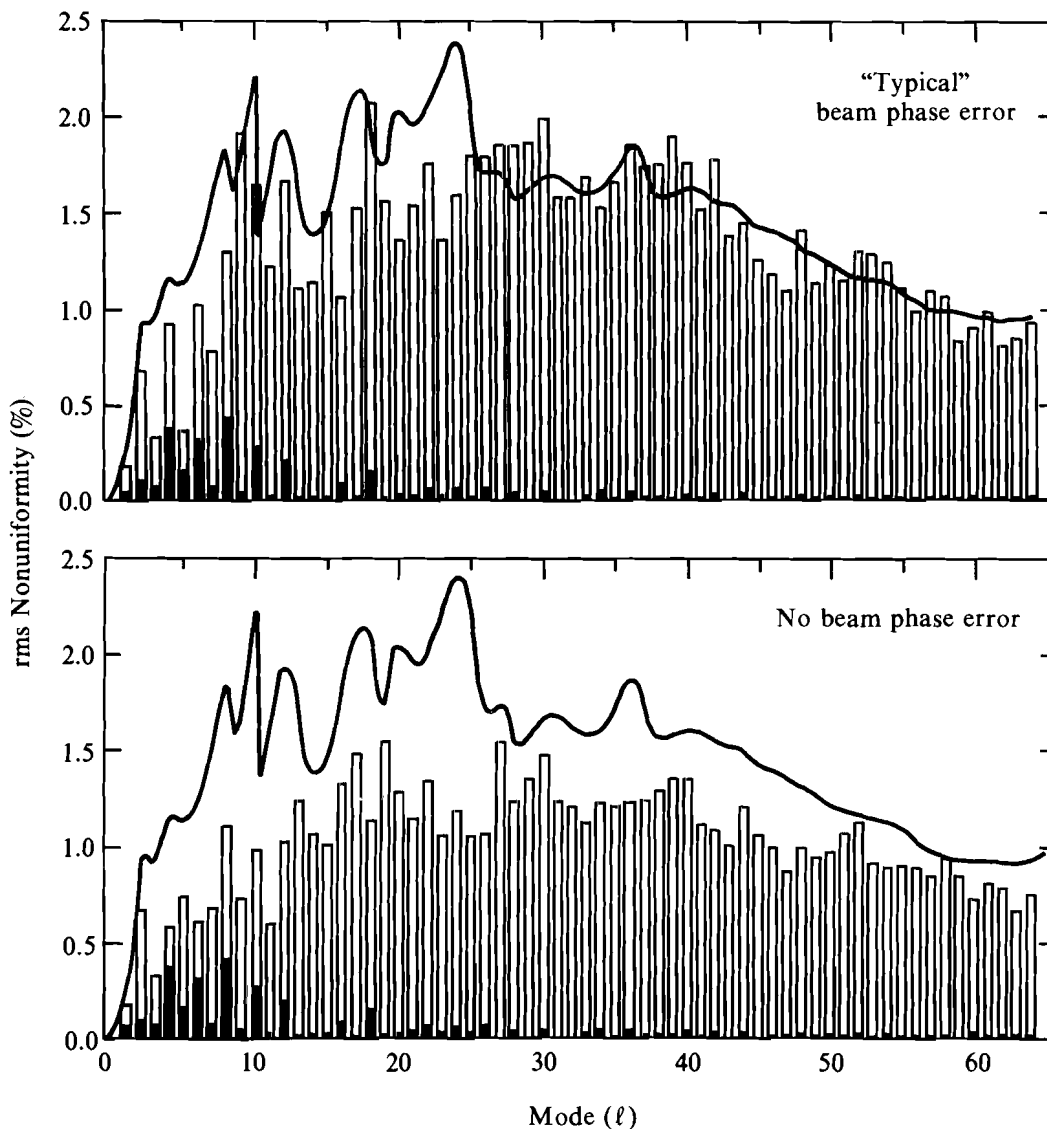
Fig. 40.17
This figure is a magnified detail of Fig. 40.16 showing that correlations in the net phase are effectively randomized by the phase error of the beam, except at the very shortest separations, over which differences in phase error are only a small fraction of a wave.

Eq. (3c) or a given n term in Eq. (4c)] is produced by element pairs closer to each other, which results in smaller differences in intrinsic beam phase between element pairs and thus less disruption of the reduced phase correlations. On the other hand, the relative amplitude of this modulation mode would be reduced by the large-number statistics of the increased number of identically displaced element pairs.

Correlation reduction represents a potentially useful complement to SSD. Even though correlation reduction would have a relatively small impact on the total nonuniformity spectrum, compared with the major degree of improvement from SSD,[5] additional reduction in nonuniformity would occur in the lowest-order modes of nonuniformity where SSD is least effective. In SSD, the reduction of nonuniformity results from averaging away the interference effects with time-varying color differences among different DPP elements. Since these color differences are smallest over the shortest separations, SSD requires the longest averaging times for smoothing the longest-scale nonuniformity. The reduction of phase correlations over these small separations would reduce long-scale nonuniformity instantaneously. Given the stringent uniformity requirements and

Fig. 40.18
To show the improvement in a simulated 24-beam illumination pattern resulting from correlation reduction, the spectrum of spherical-harmonic modes of the illumination can be compared to the solid curve, which represents an average of three simulations done with random DPP's. DPP's of 75 × 75 elements were used with a correlation-reduction range of 30 elements, and cases both with and without phase error are shown. Improvement is obtained throughout the spectrum for the case of no phase error, while significant improvement is seen only for modes up to about $\ell = 7$ for the case including phase error. The degree of deviation of the "random" curve from the mode amplitudes in the upper bar graph for the higher modes, say $\ell > 20$, is not significant. Solid bars show the mode amplitudes obtained using perfect, unmodulated beams.
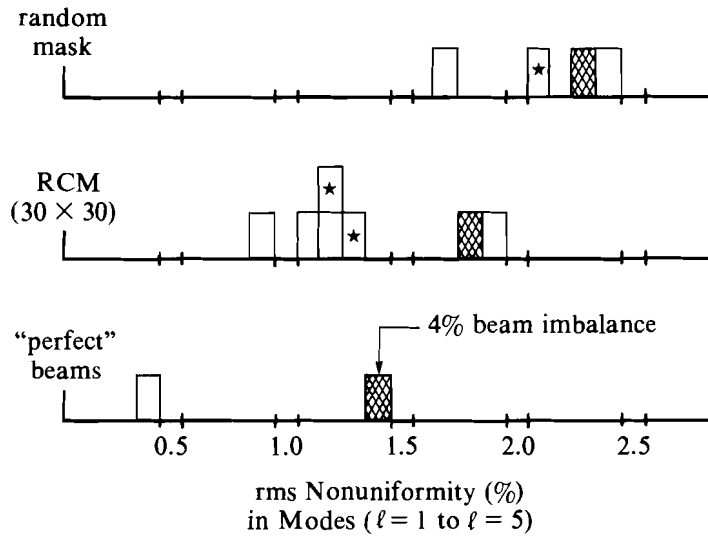
TC2586

Fig. 40.19
The consistency of improvement in the lowest modes of the simulated uniformity using reduced-correlation DPP's is seen in this set of histograms. Each rectangle represents one simulation. Simulations differ in their arbitrary initializations, the neglect of phase error (indicated by a star), or the addition of a 4% beam imbalance (shading). The simulations assume 24-beam illumination using 75 × 75 DPP's and a correlation-reduction range of 30 elements. Correlation reduction typically reduces these modes significantly closer to the level expected for perfect, unmodulated beams.

averaging-time limitations of high-compression experiments,[17] even a modest improvement of this kind could be crucial.

Reduced-correlation DPP's could be useful in holography, the original intended application of DPP's.[1] The design of lasers with low phase error would not be as constrained by the need for high power as in ICF, and more control over illumination uniformity could be exercised.

The possibility that random patterns are not optimum for DPP's is an intriguing question of principle. For improving the illumination uniformity of a focused laser beam, it is now clear that more effective patterns exist and that reduced-correlation patterns might lead to useful reductions in long-wavelength illumination nonuniformities. The degree of improvement in the spherical-illumination uniformity can range from nil to a factor-of-2 reduction in low-order modes, depending on the intrinsic phase error of the beam. For a typical level of phase error in a high-quality, high-intensity laser, such a degree of improvement might be possible. Reduced-correlation DPP's will cost no more to implement than random DPP's, and from all indications, they are virtually risk-free. At worst, they are effectively equivalent to a random mask when overwhelmed by phase error in the beam. Experiments now in progress will better determine the utility of these new patterns.

ACKNOWLEDGMENT

REFERENCES

1. C. B. Burckhardt, *Appl. Opt.* **9**, 695 (1970).

2. Y. Kato and K. Mima, *Appl. Phys. B* **29**, 186 (1982); Y. Kato *et al., Phys. Rev. Lett.* **53**, 1057 (1984).

3. LLE Review **33**, 1 (1987).

4. M. Born and E. Wolf, *Principles of Optics,* 6th corrected edition, (Pergamon Press, New York, 1980).

5. S. Skupsky, R. W. Short, T. Kessler, R. S. Craxton, S. Letzring, and J. M. Soures, to be published in *J. Appl. Phys.* See also: LLE Review **36**, 158 (1988); LLE Review **37**, 29 (1988); **37**, 40 (1988).

6. S. Skupsky and T. Kessler, *Opt. Commun.* **70**, 123 (1989). See also: LLE Review **31**, 106 (1987).

7. R. H. Lehmberg and S. P. Obenschain, *Opt. Commun.* **46**, 27 (1983).

8. Y. Takeda, Y. Oshida, and Y. Miyamura, *Appl. Opt.* **11**, 818 (1972).

9. F. J. MacWilliams and N. J. A. Sloane, *Proc. of IEEE* **64**, 1715 (1976), and references therein.

10. D. Calabro and J. K. Wolf, *Inform. and Control* **11**, 537 (1967).

11. T. M. Cannon and E. E. Fenimore, *IEEE Trans. Nucl. Sci.* **NS-25**, 184 (1978).

12. A. R. Gourlay and J. B. Stephen, *Appl. Opt.* **22**, 4042 (1983); S. R. Gottesman and E. J. Schneid, *IEEE Trans. Nucl. Sci.* **33**, 745 (1986).

13. E. E. Fenimore and T. M. Cannon, *Appl. Opt.* **17**, 337 (1978).

14. M. J. E. Golay, *J. Opt. Soc. Am.* **61**, 272 (1971).

15. W. C. Stewart, A. H. Firester, and E. C. Fox, *Appl. Opt.* **11**, 604 (1972).

16. S. Skupsky and K. Lee, *J. Appl. Phys.* **54**, 3662 (1987).

17. LLE Review **37**, 2 (1988).